Available online at www.sciencedirect.com
ScienceDirect
Coastal Engineering 54 (2007) 493–505
Coastal Engineering
An International Journal for Coastal, Harbour and Offshore Engineers
www.elsevier.com/locate/coastaleng

Application of remote sensing video systems to coastline management problems

A. Kroon [a,*], M.A. Davidson [b], S.G.J. Aarninkhof [c], R. Archetti [d], C. Armaroli [e], M. Gonzalez [f], S. Medri [d], A. Osorio [f,g], T. Aagaard [a], R.A. Holman [h], R. Spanhoff [i]

[a] Institute of Geography, Faculty of Science, University of Copenhagen, Øster Voldgade 10, 1350 Copenhagen, Denmark
[b] School of Earth, Ocean and Environmental Sciences, University of Plymouth, Drake Circus, Plymouth, Devon PL4 8AA, United Kingdom
[c] WL | Delft Hydraulics, Rotterdamseweg 185, 2629 HD Delft, The Netherlands
[d] DISTART, University of Bologna, Viale Risorgimento 2, 40136 Bologna, Italy
[e] Department of Earth Science, University of Ferrara, Via Saragat 1, 44100 Ferrara, Italy
[f] Ocean & Coastal Research Group. Departamento de Ciencias y Técnicas del Agua y del Medio Ambiente, Universidad de Cantabria, 39005 Santander, Spain
[g] Escuela de Geociencias y Medio Ambiente, Facultad de Minas, Universidad Nacional de Colombia, Medellín, Colombia
[h] College of Oceanic and Atmospheric Sciences, Oregon State University, 104 COAS Administration Building, Corvallis, OR 97331–5503, United States
[i] National Institute for Marine and Coastal Management/RIKZ, Kortenaerkade 1, 2518 AX The Hague, The Netherlands

Available online 28 February 2007

Abstract

This contribution evaluates the application of coastal video systems to monitoring and management of coastal stability problems on sandy coastlines. Specifically, video-derived parameters (coastal state indicators or CSIs) are developed which facilitate the measurement of the shoreline evolution (erosion/accretion) and response to storms, seasonal cycles and anthropogenic interventions like beach/shoreface nourishment and dredging. The primary variable which forms the basis for all the CSIs discussed in this contribution is the shoreline position derived from time-averaged video images. These waterlines are used to generate secondary products including shoreline contours at a constant pre-defined level, (intertidal) beach volumes, and momentary shoreline positions which reflect the sand volume in a meter wide section of the intertidal coast. Video-derived coastal state indicators were verified via comparisons with traditional topographical/bathymetric surveying techniques and a good agreement was found in all cases. CSIs were computed for three contrasting sandy coastal environments including an unprotected natural beach, a protected beach and a spit. Firstly, results are presented which demonstrate the advantages of coastal video systems over and above infrequent traditional topographic/bathymetric surveying methods. Namely, the ability of video-derived CSIs to quantify the magnitude, accurate location, precise timing and rates of change associated with individual extreme events and seasonal variability in the wave climate. Secondly, video-derived coastal state indicators were used to monitor two different types of human intervention, including beach nourishments and a dredged pit in a navigation channel. The video-derived datasets of coastal state indicators offered significant improvement to current CZM practices, facilitating better timing of management interventions as well as more effective monitoring of the spatial impact and longevity of these actions.

Keywords: Coastal state indicator; Argus video system; Coastline management; Waterlines; Shorelines; Beach profiles; Beach; Spit; Storm events; Beach nourishment; Shoreface nourishment; Dredging

1. Introduction

Coastal stability is an important issue along much of the world's shorelines. Many countries experience coastal safety problems and need to protect their beaches and dunes against erosion and flooding during storm events. Additionally, it is important to estimate the impact of human interventions like beach nourishments or dredging activities on the coast. Traditionally, the state (integrity) of the coast is monitored using some measure of the shoreline position and its variation in time, measured for example by successive cross-shore profiles and aerial photographs within a typical annual or biannual measurement frequency. However, the precise definition of what constitutes the coastal position varies significantly globally and the typical annual/biannual sampling frequency

* Corresponding author. Tel.: +45 35 32 25 09; fax: +45 35 32 25 01.
E-mail address: ak@geogr.ku.dk (A. Kroon).

0378-3839/$ - see front matter © 2007 Elsevier B.V. All rights reserved.
doi:10.1016/j.coastaleng.2007.01.004

is inadequate to accurately resolve the nature and magnitude of seasonal changes or the precise impact of a particular extreme event. In the past decade the potential of static, remote sensing video systems (Holman and Stanley, 2007-this edition; Turner et al., 2004; Turner and Anderson, 2007-this edition; Boak and Turner, 2005) for improved resolution of shoreline evolution in both time and space has become apparent. These video systems increase the data available for coastline management; typically sampling at least once per hour (Holman and Stanley, 2007-this edition) and they can provide long-term datasets showing variations over days, events, months, seasons and years. The video images also give detailed high resolution ($O10^0$ m) estimates of the coastal position over an area covering 1 to 5 km of coast.

The present study utilises time-averaged video images as a primary data source to derive a variety of Coastal State Indicators (CSIs) which effectively monitor the spatiotemporal evolution of the coastline and responses to human intervention. A CSI is a simple parameter which assists the monitoring and management of the coast and directly initiates management intervention when predefined threshold values are exceeded. A full description of CSIs is given in Davidson et al. (2007-this edition). CSIs under consideration here include:

- Shoreline contours measured at predefined vertical heights
- Intertidal beach volumes
- Momentary intertidal shorelines (*MICL*), reflecting the intertidal sand volume of sediment in a meter wide strip of the coast (Van Koningsveld and Mulder, 2004).

Long time series ($O10^0$ years) of these CSIs are analysed, assessing the natural variability of defended and undefended sandy coasts, thresholds beyond which management intervention should occur (see the frame of reference for coastal management issues by Van Koningsveld, 2003), as well as the impact of human interventions.

A brief description of shoreline management procedures for coastal stability problems along sandy coasts is given in the next section. This is followed by a brief overview of the field sites used in this contribution and the methodology used to derive the CSIs listed above. The resulting CSI time series are firstly computed for natural coastlines which are free from management interventions. This study examines whether video systems can resolve the magnitude, rate of change and spatial variability of the coastline to individual storm events and seasonal changes in the wave climate. Secondly, analyses of CSIs for coastlines that are subject to anthropogenic intervention are considered. This latter study assesses whether video-derived CSIs can resolve a measurable response to both beach/shoreface nourishment and dredging operations in a navigation channel. Coastal video systems are used to estimate the magnitude, rate of change, spatial coverage and longevity of both types of intervention. Finally, the benefits and applicability of the video-derived CSIs to coastal zone management practices relative to traditional management schemes are discussed.

2. Background

2.1. Shoreline management

Van Koningsveld and Mulder (2004) provide a basic frame of reference for Coastal Zone Management policy development, which explicitly shows the role of quantitative coastal state information or CSIs in relation to decision making (Fig. 1). Their framework involves the explicit definition of *strategic objective* (the overall management objective) and *operational objective* (specifically what must be done to achieve the overall management objective), for use with a 4-step decision recipe consisting of 1) a quantitative state concept, 2) a bench marking procedure, 3) a procedure for CZM interventions and 4) an evaluation procedure. A full description of this process may be found in Davidson et al. (2007-this edition) and therefore no further detail is provided here. The key component of this approach is the CSI. Presently, the main CSI in the case of shoreline management is the shoreline position. Worldwide, the shoreline position is defined in many ways as reviewed by Boak and Turner (2005). Quite often, cross-shore profiles, aerial photographs and/or Lidar observations (e.g., Stockdon et al., 2002; Sallenger et al., 2003) are the main source to evaluate the coastline stability. The sampling frequency of most of these data sources is typically once or twice a year and surveys are always made during low-energy wave conditions reducing their value for studies of storm impact.

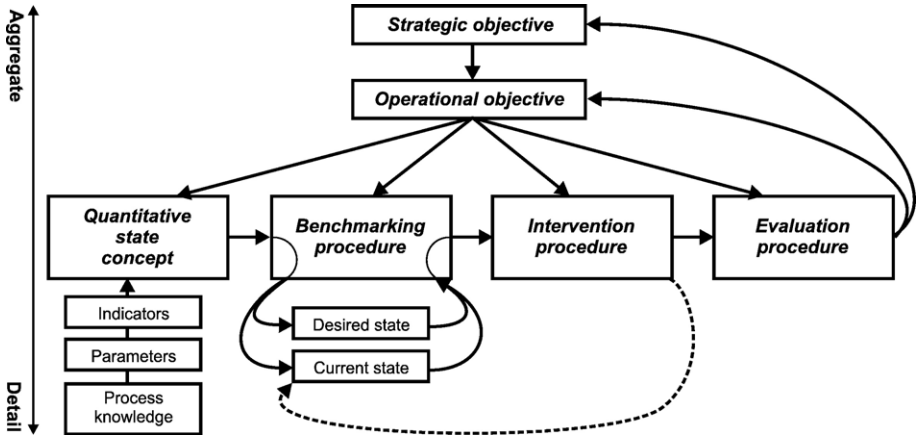

Fig. 1. Basic frame of reference as a tool for Coastal Zone Management policy development (after Van Koningsveld and Mulder, 2004).

An operational (Dutch) CSI for coastal protection from flooding that is discussed later in this paper in relation to a video-derived analogue is the Momentary Coastline (*MCL*), an aggregated measure for the location of the low-tide beach contour. The *MCL* position is determined from a nearshore sand volume as observed from annual surveys of beach and surf zone bathymetry (see Van Koningsveld and Mulder, 2004). The upper boundary of the *MCL* position is the dune foot and the lower boundary is defined as the local low-tide level minus the height between dune foot and low-tide level. The landward boundary of the *MCL* position is a reference line in the dune area. Time series of the *MCL* position at a specific location give an indication of the coastline trend over years. The natural variability of the *MCL* position within a year, due to the impact of storms or other seasonal effects is still unknown. Coastal managers intervene when the *MCL* position falls below a critical threshold value, the *BCL* (Basic Coastline) position. In the Netherlands, the *BCL* is for instance based on the coastline position in 1990. These interventions are generally beach and/or shoreface nourishments (Hamm et al., 2002).

2.2. Beach nourishments and dredging activities

Beach and shoreface nourishments are commonly implemented by coastal managers to protect sandy coastlines against erosion (e.g., Hamm et al., 2002; Hanson et al., 2002). The direct effect of the nourishment is an extra volume of sediment in the specific area that serves as an additional sediment buffer combating storm erosion. Indirect effects of shoreface nourishments are the increased dissipation of wave energy over the shallow areas and the stimulation of onshore directed sediment transport flux by asymmetric waves during low- to moderate-wave energy conditions (Spanhoff et al., 1997, Van Duin et al., 2004). After nourishment, additional data are needed to monitor the life-time of the nourishment, and thus its success (or otherwise). In Holland for example, nourishments are traditionally monitored with a sampling frequency of 2 to 3 times per year over several years. Additional values of the *MCL* position are computed and used to compute the life-time of the nourishment which is defined as the period starting from the initiation of the nourishment works to the next crossing of a *BCL* position. These monitoring schemes seem barely adequate to describe the evolution of shoreface nourishments, and are too infrequent to determine the life-time of beach nourishments with accuracy. Moreover, it is impossible to assess the detailed processes that cause the shifts in the evolutionary trends of the nourished areas.

The physical impacts of dredging on shoreline change have been recognized worldwide (e.g., Horikawa et al., 1977; Bender, 2001; Simons and Hollingham, 2001; Work et al., 2004). A direct effect of dredging is the cross-shore sediment transport into the dredged pit, which appears as a net loss of sediment from the dry beach (Demir et al., 2004). An indirect effect arises from the wave refraction generated by the pit, which modifies the wave heights and directions, and thus changes the alongshore sediment transport pattern and shoreline position. The decision to intervene in the natural evolution of a spit system often depends on the movement of the spit end into the navigation channel. Traditionally, cross-shore profiles are used to determine the evolution of a spit end by monitoring the slope of the channel and the location of the slope break in the profile. This decision heavily relies on the sampling frequency of the cross-shore profiles.

2.3. Shoreline management and video-derived CSIs

Coastal management decisions to nourish a beach or dredge a shipping channel are based on comparing the state of the system with a pre-defined threshold value. This process requires a methodology for returning long-term, high-frequency measurements of coastal state. Long-time series are required in order to separate the natural (e.g., seasonal) variability of a system from longer-term trends in erosion or accretion, and very importantly from a management point of view, to establish appropriate threshold conditions for intervention. The high-frequency measurements are required in order to resolve unaliased trends in the CSI time series and to initiate timely intervention procedures where it is a policy to do so. After the introduction to the different field sites used in this contribution, the potential contribution of video monitoring techniques to policy development cycles by means of the quantitative assessment of CSIs (step 1 of the basic frame of reference, Fig. 1) is investigated. Here there are three possible ways of proceeding: 1) by establishing video-derived CSIs which directly replicate existing indicators and fit directly into current frames of reference (e.g., the *MCL*), or 2) by establishing new video analogues for established CSIs (e.g., the *MICL*) which also match existing operational objectives, or 3) by establishing completely new CSIs which cater for entirely new operational objectives. The latter is appropriate where video systems demonstrate the possibility of enhancing management practices which were not previously possible with conventional measurement systems.

3. Field sites and video systems

This section is limited to a brief description of the CoastView field sites, a more detailed description can be found in Davidson et al. (2007-this edition). Three sandy beaches with Argus video systems were used to detect the shoreline position CSI, its variability in time and its applicability in management schemes. The sites were located in Egmond in the Netherlands, Lido di Dante in Italy and El Puntal in Spain (Fig. 2). The wave and tidal information relating to these sites are summarized in Table 1.

The Egmond site is a sandy beach with dunes and a barred nearshore zone. The nearshore bars show a sequential behaviour of O(15 years) with initiation near the low waterline, migration offshore and destruction in the outer nearshore (see e.g., Ruessink and Kroon, 1994; Wijnberg and Terwindt, 1995). The intertidal bars show a sequential behaviour of O(months) (Kroon et al., 2002) with initiation near the low waterline, migration onshore during calm conditions and increasing mean high-water levels, and merging to the beach (extra net-sediment

accumulation) or erosion during a storm event (c.f. Wijnberg and Kroon, 2002). The intertidal bars closely follows the shoreline configuration which is often rhythmic with mega-cusps having a spacing of O(500 m) (see Aagaard et al., 2005). The Egmond site suffers from erosion and regular nourishments have been performed since 1990.

The Lido di Dante beach (Fig. 2) stretches between the Fiumi Uniti and the Bevano rivers. The northern, 1 km long stretch of beach is protected by three groins and a semi-submerged breakwater (crest height = MSL), and the southern 2 km long beach is a natural stretch of coastline with a dune field and a complicated and highly dynamic sub-aqueous crescentic bar system with rips. The protected beach suffered from erosion before its construction works started. The northern part of the unprotected beach retreated in the period 1978–1996, due to the southern groin of the protected beach (Ciavola et al., 2003). Over the same period, the beach between 750 and 1700 m from the groin retreated up to 1982 and showed

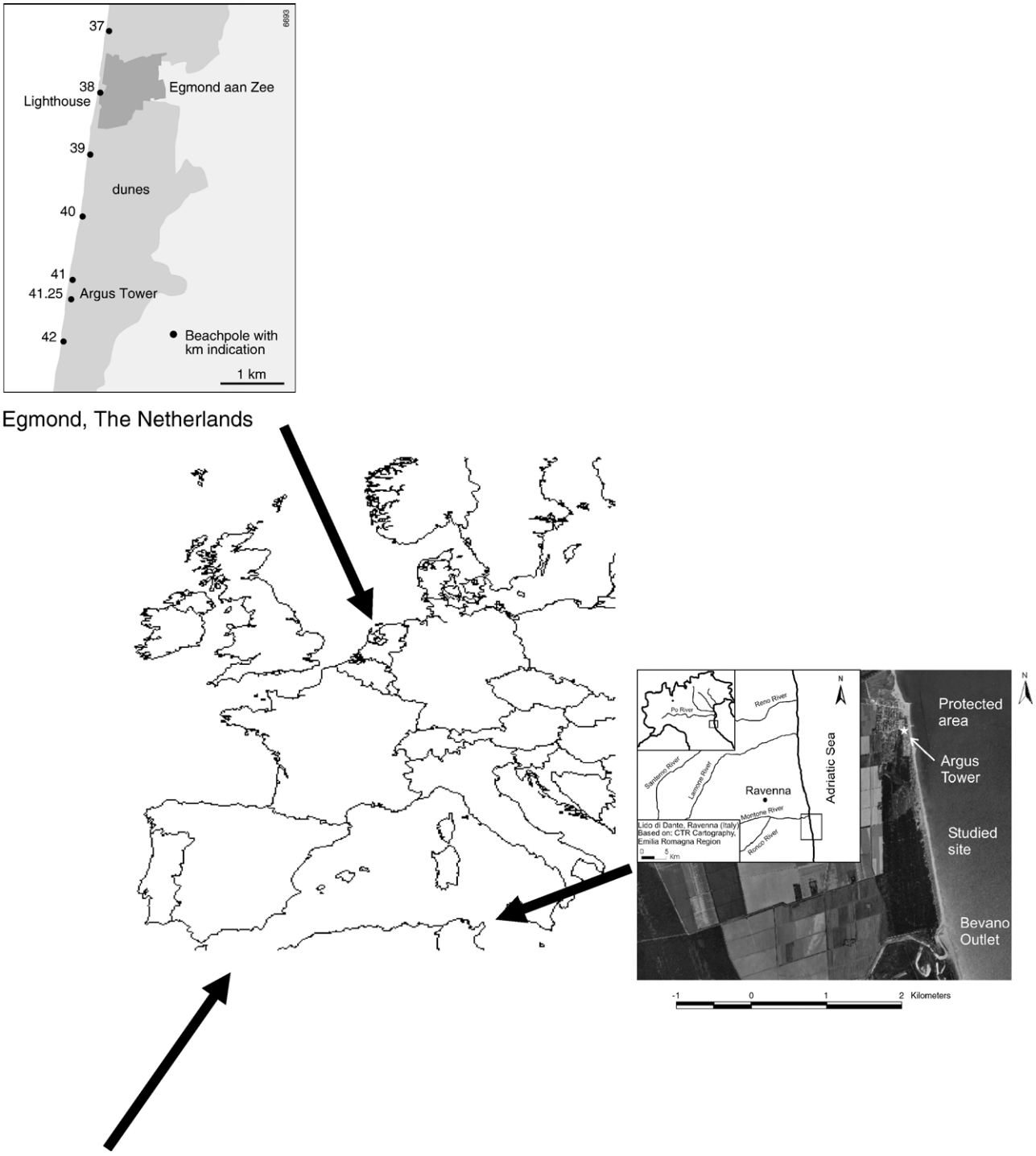

Fig. 2. Field sites at Egmond, Lido di Dante and El Puntal.

Fig. 2 (*continued*).

accretion between 1982 and 1996. Further to the South, the beach slowly advanced in the area next to the Bevano River (Fig. 2). Several nourishments were placed in front of the protected area (60,000 m^3 in 1993 and 74,400 m^3 in 1996) and smaller nourishments inside the structures were regularly implemented to increase beach width for beach users in the summer season.

The El Puntal spit is a 2.5 km long stretch of beach with dunes and is located in the Bay of Santander. Its northern shore faces the Atlantic Ocean. The wave height along the spit from the central part to the western tip of the spit decreases due to diffraction and refraction effects caused by the shelter effect of Magdalena Peninsula (Fig. 2). The alongshore gradients in wave height drive strong longshore currents and sediment towards the tip of the spit. Maximum wave heights at the end of the spit are predominantly < 1.0 m and mean wave conditions do not normally induce a significant alongshore current here. Maximum values of ebb and flood tidal currents near the spit end are typically about 1.0 m/s. The sheltered beach of the spit on the landward side is macro tidal and reflective. Conversely, the exposed beach is dissipative with alongshore and transverse submerged bars. The profiles at the spit end conserve a constant underwater slope of about 1:5, close to the angle of repose and sandbars are not present. Profiles here typically migrate seaward or landward without changing shape. Historic land reclamation works reduced the original Santander bay area by 50% (in the last 200 years) and its tidal prism (and currents) drastically. This reduction caused spit growth and induced a narrowing of the tidal discharge channel at the bay's mouth. In order to maintain a safe navigable channel the end of the spit must now be constrained from further migrating and is constantly dredged to a depth of 15 m (see Losada et al., 1991). Currently the Santander Port Authority dredges between 50,000 and 100,000 m^3 of sediment per year from the bay mouth (spit end) and pumps it to the central area of the beach (Medina et al., 2007-this edition).

Video measurements at the CoastView sites are based on the use of Argus Stations (see Holman and Stanley, 2007-this edition). The characteristics of these sites are summarised in Table 2.

4. Methods

All CSIs presented here were based on video-derived shoreline positions. Time-exposure images (10 min time averages) were used to estimate waterline positions and to compute intertidal beach bathymetries and intertidal momentary coastline positions. The simplest way to derive a waterline was to merge and rectify video images of the different cameras to create one plan view image (see e.g., Lippmann and Holman, 1989; Holland et al., 1997) and further digitize the waterline. A more sophisticated method quantified waterlines and intertidal beach bathymetries with the help of the Intertidal Beach Mapper (Aarninkhof et al., 2003). This was achieved by mapping a series of beach contours, sampled throughout a tidal cycle. The mapper delineated a shoreline feature from time-averaged video imagery on the basis of the visual contrast between the sub-aerial and sub-aqueous parts of the beach

Table 1
Shoreline orientation, waves, tides and sediment characteristics of the field sites

	Egmond	Lido di Dante	El Puntal
Shoreline orientation	7° N–S	N–S	E–W
Annual wave height and period	1.3 m; 5 s		1.0 m
Storm waves	3.5–5 m; 8 s		5 m; 16 s
Preferential wave direction	SW–NW	Storms from 'Scirocco' (60°–120°); highest waves from 'Bora' (0°–60°)	75% from N–NW
Tide	Semi-diurnal	Semi-diurnal	Semi-diurnal
Neap range	1.4 m	0.3 m	
Mean range			3 m
Spring range	2.1 m	0.8 m	5 m
Mean grain size of sediments	0.25 mm		0.30 mm

Table 2
Characteristics of the video systems at the field sites

	Egmond Argus Tower	Egmond Light House	Lido di Dante Argus Tower	Santander Hotel Real
Installation	April 1998	May 1999	February 2003	March 2003
Height above mean sea level	40 m	43 m	20 m	90 m
Main focus	Sandy unprotected beach	Sandy unprotected beach	Sandy protected and unprotected beach	Sandy beach on spit
Alongshore stretch	3 km	3 km	1 km and 2 km	2 km
Pixel resolution				
Cross-shore	0.5 m	0.5 m	0.5 m	0.5 m
Alongshore	0.5–2.0 m	0.5–2.0 m	0.5–2.0 m	0.5–2.0 m
Burst interval between images	60 min	60 min	60 min	30 min
Argus system (Holman and Stanley, 2007-this edition)	Argus II	Argus II	Argus III	Argus III

(waterline detection). The corresponding shoreline elevation was estimated with the use of local water levels and wave conditions at the time of image collections (see Aarninkhof et al., 2003), assuming an appropriate foreshore beach slope. The computed bathymetric maps were interpolated to a rectangular grid with a resolution of 5 m (20 m) in the cross-(along-) shore direction, using an advanced quadratic Loess interpolator (Plant et al., 2002).

The mapped shoreline elevations on the intertidal beach were further used to characterise a standard measure for the shoreline position (the CSI). This was done by defining the shoreline position at a specific standard water level or by determining a new CSI, the momentary intertidal coastline position (*MICL* position). The *MICL* position is an analogue of the *MCL* position, but based on volumes in the intertidal part of the beach with the upper boundary at MSL+1 m and the lower boundary at MSL (this level was always visible in the images). Wijnberg et al. (2004) conducted a ground truth procedure between the video-derived *MICL* values with a longshore spacing of 20 m and *MICL* values based on traditionally surveyed intertidal beach profiles. A good correlation with systematic differences between the two was found. Occasionally, *MICL* position values could not be determined because of missing values in the interpolated bathymetry when local interpolation errors were too large due to a lack of nearby data points. For the analyses presented herein, missing *MICL* position values were filled by linear interpolation in the longshore direction.

The accuracy of the Intertidal Beach Mapper is discussed in detail in Aarninkhof (2003) and Aarninkhof et al. (2000, 2003). These include errors related to blurred images induced by atmospheric disturbances, like mist, rain and clouds, bright excess of foam in the surf zone and overexposure due to sunset or sunrise. Other errors included those induced by poor horizontal and vertical camera resolution, which worsen with distance from the camera (Holman et al., 1993). Further errors in the video-derived bathymetry could occur due to longshore pressure gradients resulting from strong tidal currents near a spit end for example (Siegle et al., 2002), or longshore pressure gradients associated with irregular barred nearshore topography or variations in beach slope. Some of these errors can be removed by a combined use of elevation models and numerical hydrodynamic models (Plant and Holman, 1997; Siegle et al., 2002; Aarninkhof, 2003; Smit et al., 2007-this edition).

5. Results

5.1. Shoreline positions, impact of storms and long-term evolution

5.1.1. Storm responses

Neither the impact of extreme events nor seasonal cycles in coastal evolution are adequately measured using the relatively infrequent traditional methods for evaluating coastal state. Here results are presented which illustrate the impact of storms on the shoreline configuration for each of the field locations under consideration.

5.1.1.1. Egmond, the Netherlands. A presentation of the evolution of video-derived, low-tide waterlines during a storm event is presented in Fig. 3 (see also Aagaard et al., 2005), together with the offshore root-mean-square wave heights (H_{rms}) and surge levels during October 2002 at Egmond. H_{rms} values exceeded 6 m on the 27 October 2002. The strong crescentic pattern in the low-tide waterline which was observed prior to the storm was reduced in amplitude from 20–30 m to 10–20 m. However, the morphological pattern was not completely reset which was also observed for similar scale patterns in nearshore bar alignments by Van Enckevort and Ruessink (2003). The mean alongshore position of the low-tide line remained spatially unchanged, despite the volumetric loss of sediments from the supratidal and upper intertidal beach towards the lower intertidal beach and inner nearshore (not shown). The intertidal beach slowly recovered under low-energetic wave conditions in the weeks after the storm and the alternation of horns and embayments remained in place.

5.1.1.2. Lido di Dante, Italy. A storm on 24–27 September 2004 at Lido di Dante was characterised by north easterly waves with H_{rms} exceeding 2 m for 12 h, with a peak period of 7 s and maximum storm surge levels of 0.7 m (measured in nearby Ravenna). The video-derived (mean water level) shoreline position and its changes during spring tide conditions around the storm are presented in Fig. 4. The shoreline response was an erosive area close to the groins (with a retreat of −4 to −7 m), a less erosive central region, and a stable or accreting section furthest from the Argus tower (shoreline migration of between −4 and +2 m). These patterns were in line with changes in traditionally surveyed dune foot positions over this period. Unlike the previous Egmond example the crenulated features, horns or irregularities, appear to migrate alongshore. Further evidence for the alongshore migration of these features was widespread throughout the whole image database which showed propagations in both directions. It is postulated that the horns in the mean shoreline position could be forced by the

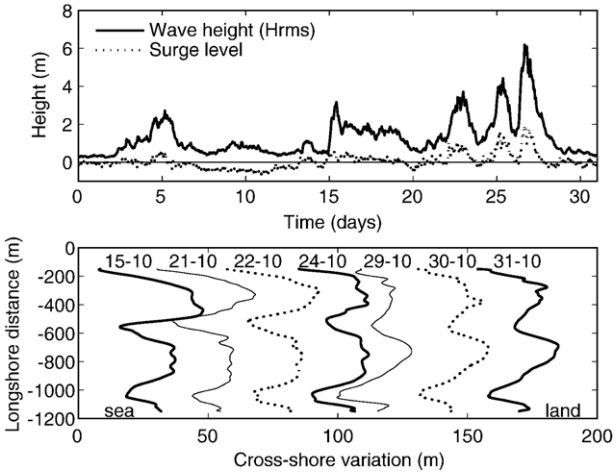

Fig. 3. Offshore wave heights (H_{rms}) and measured surge levels in October 2002 (upper panel); evolution of coastlines of a longshore stretch at Egmond beach (lower panel). Each of the successive shorelines is offset by 25 m. Note the major storm event at 27-10.

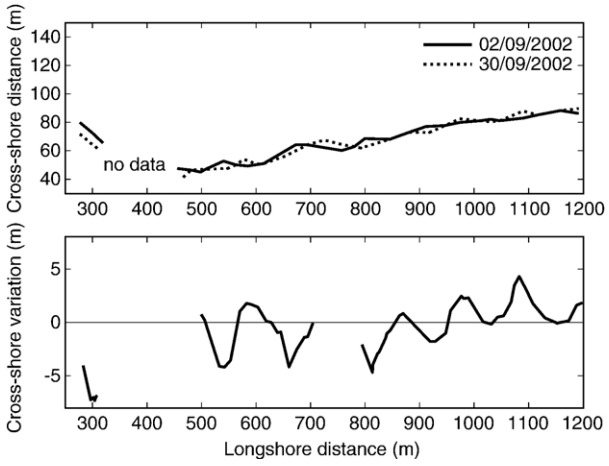

Fig. 4. Storm impact on the unprotected beach of Lido di Dante with the positions of the mean shoreline on the 2 and 30 September 2004 (upper panel) and the cross-shore variation in mean shoreline position between 2 and 30 September 2004 (lower panel). The Argus tower is at the longshore distance of 0 m and the most southern groin of the protected beach at the longshore distance of 250 m.

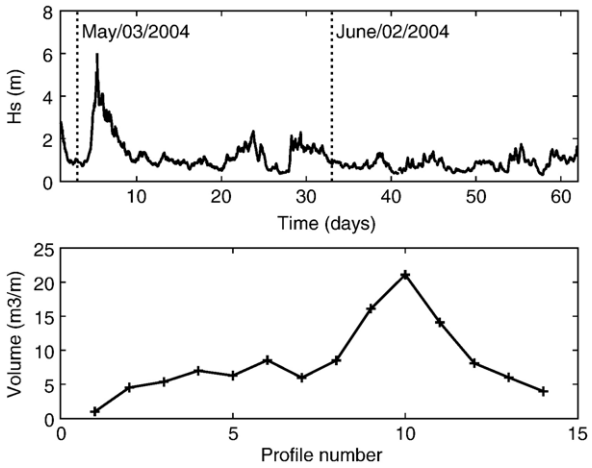

Fig. 5. Offshore wave heights (H_s) around the major storm event (upper panel) and the estimated volume of sand accumulated along the spit end of El Puntal after the storm (lower panel).

presence and/or movement of submerged morphologies, with associated rip current circulation patterns. The protected beach did not show a net loss of sediment during this event. However, its morphologic response was a displacement of sediment from the northern to the southern parts between the groins, with a flattening of the cross-shore profiles. Other storms from the SE (not shown here) showed the reverse evolutionary trends.

5.1.1.3. El Puntal, Spain. A more sophisticated CSI developed to monitor the impact of a storm is the video-derived sediment volumes. At El Puntal, the video-based intertidal beach profiles are combined with the robust assumption (for this area) that the sub-tidal slope is constant. This constant slope in the sub-tidal profile is maintained close to the angle of repose due to the scouring effect of strong tidal currents. The assumption of constant offshore slope allows the computation of the sediment budgets along the spit including sub-tidal water depths. Time series of significant wave heights over the storm period (reaching up to 6 m) and the alongshore estimated volumetric change along the spit are presented in Fig. 5. The volumetric change (Fig. 5, lower panel) is presented along 14 consecutive profiles, spaced approximately 20 m apart, where profile 1 is located in the sheltered (harbour) side of the spit, profile 3 is at the end of the spit and profiles 4–14 are located progressively eastwards on the exposed side of the spit. Typically, at this location strong longshore gradients in wave height which arise due to the sheltering effect of Magdelana Peninsula drive longshore currents and sediment towards the tip of the spit. The video estimates of the volumetric change are clearly able to quantify the magnitude and distribution of this effect with most of the sediment accumulated at the central part of the spit end where the intertidal zone advanced measurably seaward (profile 10, close to the navigation channel). At the same time, the impact of the storm was minimal at profiles 1 and 14, with little sediment accumulation. The total volume of sediment that accumulated after the storm along the spit end was estimated at about 5000 m^3.

5.1.2. Annual variability in CSIs

In this section longer time series (O(1 year)) of CSIs (typically shoreline positions) are presented in order to assess the seasonal variability in the shoreline response.

5.1.2.1. Lido di Dante. The evolution of the alongshore averaged shorelines of a protected beach in 2004 is presented in Fig. 6. The cross-shore variations of video-derived shorelines in the defended coastline were very small, the overall displacement was of O(1 m), and the observed trend indicated that the coastline was stable. This is in contrast to the previously examined storm response of the shorelines in the adjacent unprotected area which showed variations in excess of ±5 m. The combination of the storm response and longer time series provides a clear indication that although sediment is moving

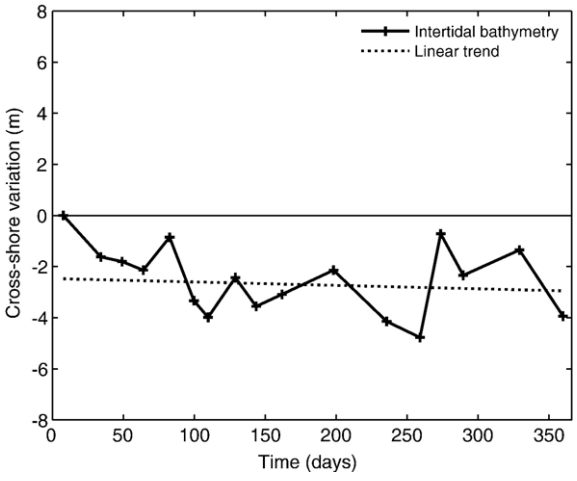

Fig. 6. Mean shoreline evolution during 2004 at the protected part of the Lido di Dante beach. The yearly averaged trend shows hardly any change over the year. Error bars around the video-derived estimations of the shoreline with the Intertidal Beach Mapper are 1.4 m.

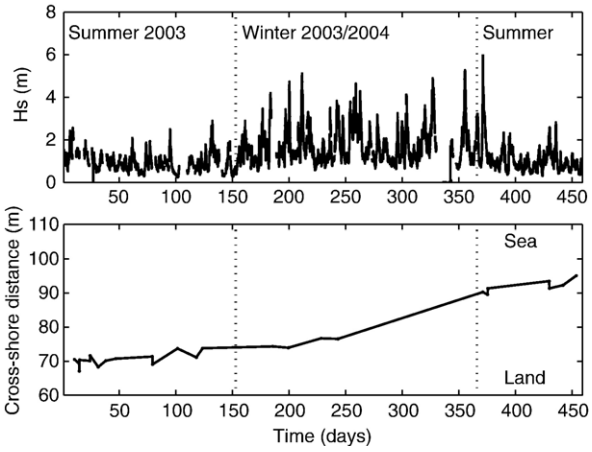

Fig. 7. Offshore wave heights (H_s) from 1 May 2003 until 31 July 2004 (upper panel) and the evolution of shorelines at the El Puntal spit (profile 12; lower panel).

around within the groin embayments during storms in the protected area of the beach, overall the coastal protection scheme is effective and very little sediment is lost or gained from this sub-system.

5.1.2.2. El Puntal. The shoreline changes of a coastal spit over a 14 month period (from May 2003 to August 2004) are presented in Fig. 7, together with the offshore significant wave height. The shoreline, defined here as the horizontal location of mean sea level measured near the tip of the spit (profile 12), did not change much in the summer season during low wave conditions. However, after major storms in October, the coastal video system was able to resolve a steady seaward shoreline movement of approximately 15 m over the winter season, (approximately 2 m/month), in the direction of the navigation channel.

5.1.2.3. Egmond. A newly derived CSI the *MICL* position, based on the intertidal beach volume, was applied to investigate the natural behaviour of the coastline of a sandy beach on time scales ranging from days to years (Wijnberg et al., 2004; Fig. 8). The similarity in values for the traditional *MCL* position and the *MICL* position in the cross-shore profile at about 650 m from the camera was striking. Most of the data points of the traditional CSI matched the video-derived CSI. However, the variations over time differed. The variation of the *MICL* position over 2 years (solid line) was of order 50 m, more than twice the value of the trend over this period. In general, the cross-shore position migrated closer to the dune foot towards the winter season and retreated seaward during the spring. Neither the seasonal pattern nor the magnitude of variation was resolved by the traditionally derived, more sparsely sampled, *MCL* position (open dots). Similar results were observed for other cross-shore transects in the video images.

5.2. Shoreline positions and the impact of beach nourishments

In this section video-derived CSIs are used to estimate the spatial impact and longevity of a beach nourishment scheme at Egmond again using a video-derived analogue of the *MCL* (the *MICL*). At this location beach erosion was serious enough to exceed the predefined benchmark value (the Basal Coastline or *BCL*), requiring the predefined intervention by means of a nourishment scheme. The coastal management scheme (or frame of reference) for these specific nourishments is presented in Fig. 9.

Two beach nourishments were executed at Egmond beach to mitigate local beach erosion. The first took place in the early summer of 1999, when a combined beach and shoreface nourishment was completed, depositing 200 m^3/m of sediment on the beach over a longshore distance of 1500 m. A further 400 m^3/m of sediment was positioned on the shoreface at a depth of 5 m, on the seaward side of the outer bar, covering a distance of 2200 m alongshore. Persistent erosion forced the authorities to place a further 260 m^3/m of sediment on the beach over a distance of 800 m alongshore in June 2000 (see Fig. 10, after Aarninkhof et al., 2003).

Video-derived intertidal beach profiles, made with the Intertidal Beach Mapper, and shorelines at mean sea level were used to evaluate the coastal response to the nourishments. These coastal indicators were monthly derived between June 1999 and August 2001. Time series of wave height and plan view intertidal beach configurations are presented in Fig. 10. During the summer of 1999, the beach in the northern part (negative y values) was much wider than in the southern part (positive y values) and the configuration looked skewed in an alongshore direction. This skewness remained until the nourishment work in July 2000. Thereafter, the beach width slowly reduced along the whole area and reached a critical width after some high-energy wave conditions over the winter months in 2000. After March 2000, the intertidal beach width showed only a slight recovery by natural processes like onshore intertidal bar migration under low-energetic wave conditions. The beach nourishment clearly widened the intertidal beach and initially centred the whole beach width pattern at the core of the nourishment in front of the village (at y values of zero). However, the beach width reduced again after October 2000 due to the increase of the wave energy over winter months, and the skewed alongshore pattern reappeared with the widest beaches again at about $y = -300$ m. The persistence of this alongshore crescentic pattern with a scale over 500 m was also observed in case of storm impacts (Fig. 3) and was probably strongly forced by the configuration of the bars in the nearshore. The life-time

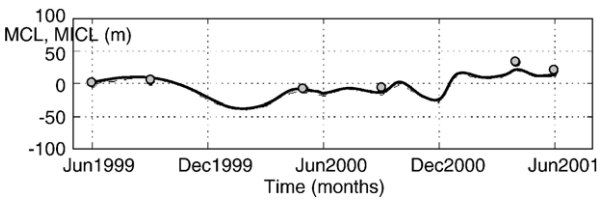

Fig. 8. Evolution of the Momentary Intertidal Coastline position (*MICL*, solid line) and the corresponding Momentary Coastline position (*MCL*, dots). Data are sampled along a cross-shore array at 650 m north of the Egmond Jan van Speijk light house. *MICL* positions are determined from Argus video imagery on a monthly basis. Both *MICL* and *MCL* time series are normalized with respect to their positions in June 1999.

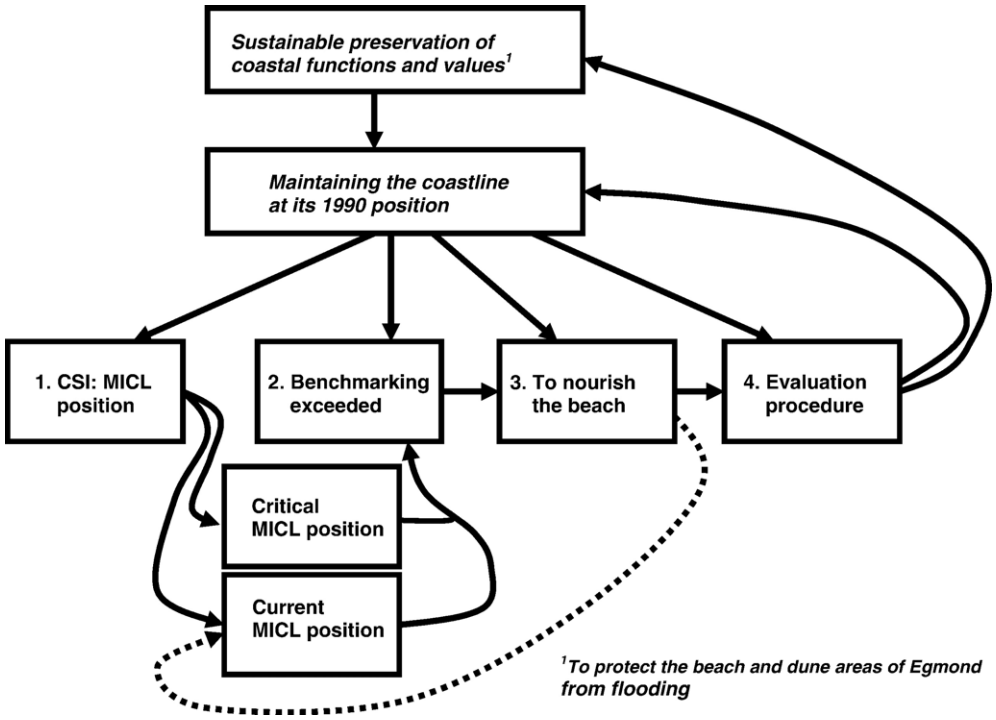

Fig. 9. Coastal stability problems and coastline management with respect to the frame of reference (Van Koningsveld, 2003): example of the beach nourishment at Egmond, The Netherlands.

of this beach nourishment was in the order of 4–6 months, based on a comparison between the pre-nourished situation in June 2000 with a similar pattern and alongshore width distribution in December 2000.

5.3. Shoreline positions and the impact of dredging activities

The effect of dredging activities on the shoreline configuration was estimated on the sandy spit of El Puntal. Here, the spit tended to migrate in to the navigation channel compromising navigational safety. The harbour authorities must ensure that the minimum depth of the channel is not below a benchmark value of 15 m. A dredging programme is in place to maintain channel tolerances. The coastal management scheme for this is presented in Fig. 11. The impacts of dredging activities on the coastline include a direct effect of cross-shore transport related sand loss into the pit, and an indirect effect of modified wave heights and directions, due to wave refraction over the pit. This changed the alongshore sediment transport pattern, and therefore shoreline position. However, the latter aspect was of less importance, due to the sheltered area of the spit.

One 5-day dredging intervention by the Port Authority at the end of the El Puntal spit was subsequently monitored in order to evaluate any corresponding shoreline response. The operation was executed between 26 and 30 April 2003 and the dredged volume of sediment was approximately 48,000 m^3 (240 m^3/m). The location and dimension of the dredge pit are shown in Fig. 12.

The video-derived shoreline at mean water level was used as a CSI, and the objective was to quantify the maximum retreat of the shoreline and alongshore extent of the zone affected. The evolution of mean sea level contour near the end of the spit over months around and after the dredging activity is presented in Fig. 12. At the eastern part of the spit end, the shoreline presented small variations over the year (P1). However, a bit further towards the end of the spit, the shoreline was initially quite stable and showed a seaward shift during the storm season in the winter after the dredge (P3). The shoreline at the location of the dredged pit (P4) showed an initial retreat of about 15 m in the first month, followed by a slow retreat over the next 6 months in which total retreat was about 30 m. Subsequently, the shoreline showed a seaward migration during the storm season in the winter after the dredge with sediment transported alongshore from the central beaches of the spit. The behaviour of the shoreline at the end of the spit is similar to the previous location. However, the rates are less and the total retreat in the first 6 months was about 15 m. The impact of the dredging was clearly observed behind the dredged pit up to the spit end. The effect of the dredged volume on the shoreline configuration was however less than a year. The shoreline once again protruded into the channel after the stormy winter season of 2003–2004.

6. Discussion

This paper has examined the potential of coastal video systems for providing state indicators that assist coastal managers in the monitoring and management of coastal stability problems. All the indicators discussed here are based on the detection and rectification of the shoreline position derived from time-averaged images. Tertiary products which are subsequently

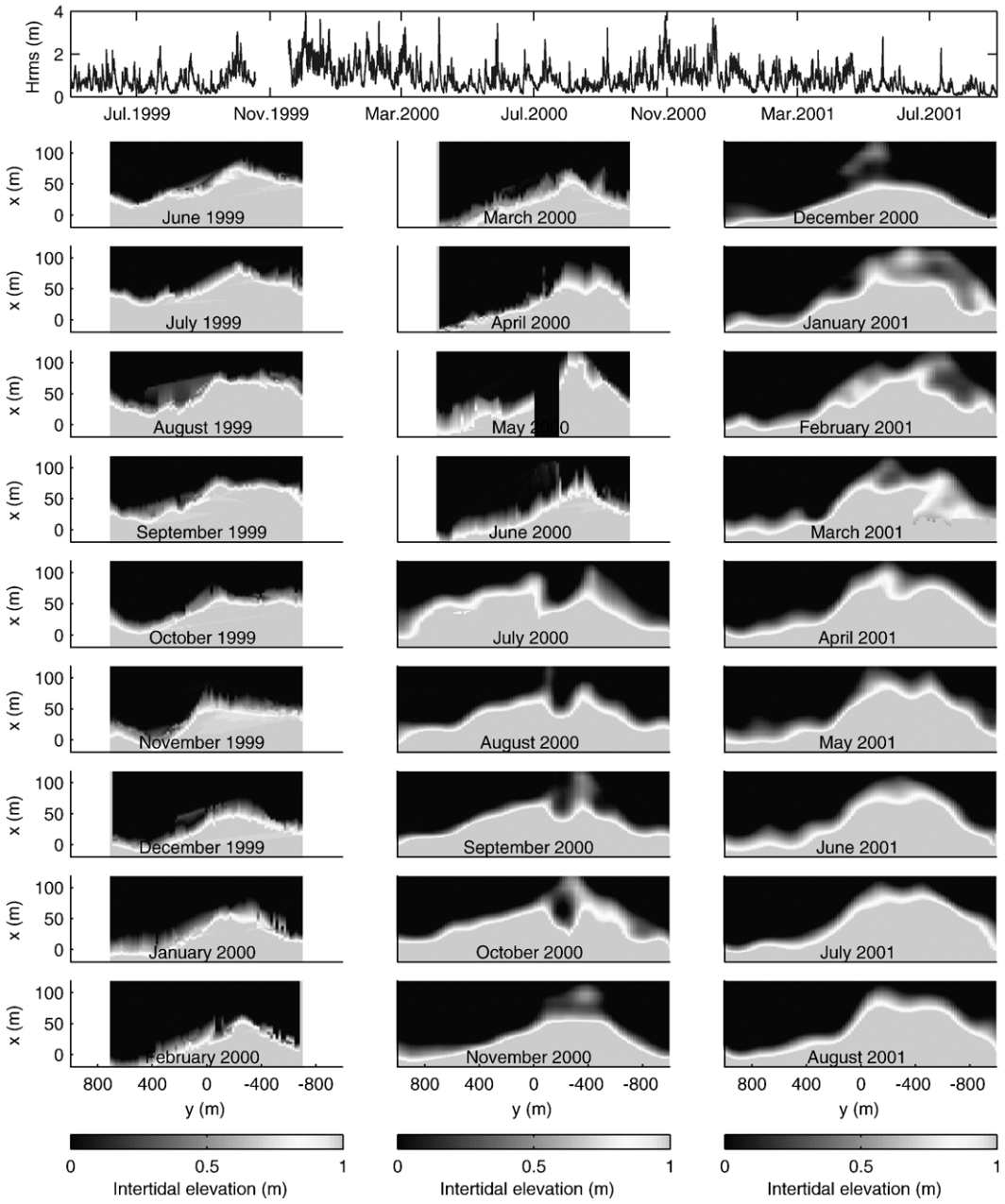

Fig. 10. Offshore wave heights (H_{rms}) at Egmond from June 1999 to August 2001 (upper panel) and the monthly evolution of the shoreline derived from Argus video images of the intertidal beach over the same 2 years (lower panels). Note the change after the nourishment in July 2000.

used as indicators include, shoreline contours at predefined vertical elevations (e.g., mean sea level), intertidal beach volumes/volumetric changes, and the momentary coastline position.

In all cases these parameters were seen to be effective in quantifying the magnitude, precise timing and spatial distributions of storm responses and seasonal variations in the shoreline position. The spatial and temporal impact and longevity of interventions was also successfully monitored using video-derived CSIs. These methodologies exceed the capability of traditional direct measurement techniques. In all cases the measured signals were significantly larger than the uncertainty associated with the indicators.

The video-derived intertidal beach morphologies and shorelines were compared to traditionally levelled profiles. In most cases, the correlation was excellent: Video-derived intertidal beach slopes and traditionally levelled beach slopes at Lido di Dante were found to be the same. Video-derived profiles and traditionally levelled profiles (DGPS/GPS system) over a 2 km sandy beach on the El Puntal spit showed similar results. Over 4 days (24 September 2003, 3 May, 2 June and 2 July 2004) there was a mean bias of 0.36 m and a standard deviation of 0.10 m. Expressed in terms of horizontal deviations, the bias was 3.6 m with a standard deviation of 0.85 m. The total estimated error in the calculation of the accumulated sediment volume during the previous described

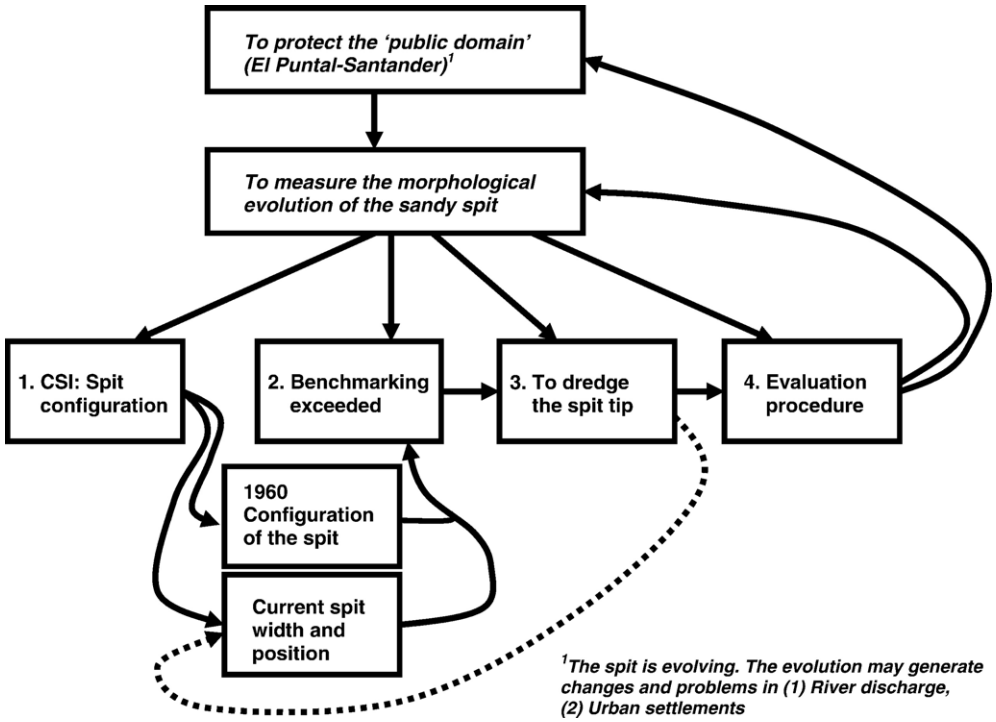

Fig. 11. Coastal stability problems and navigation management with respect to the frame of reference (Van Koningsveld, 2003): example of the dredge site at Santander, Spain.

storm event was 4% (200 m^3 of 5000 m^3). The *MICL* position was an aggregated measure for the shoreline position which showed a very robust comparison to its analogue the *MCL* derived from traditional surveys (Fig. 8). The *MICL* and *MCL* together with estimates of volume are thought to be a more robust measure of coastal state than the individual shoreline contour time series. For example, the mean alongshore position of the low-tide line remained almost in the same place during the Egmond storm analysis, despite the volumetric loss of sediments from the supratidal and upper intertidal beach. The indicators based on volume would provide a more robust reflection of this erosion than a single contour line.

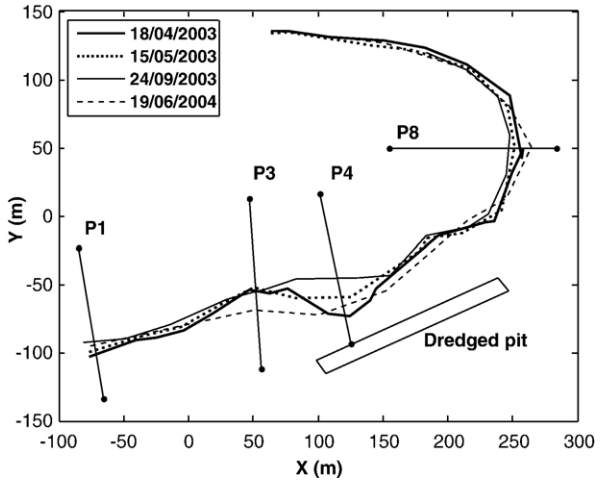

Fig. 12. Evolution of the shoreline associated with the mean sea level for profiles P1, P3, P4 and P8. The dredged pit is about 200 m by 40 m and its volume is about 48,000 m^3. The pit was dregded at 24 April 2003. Initial shoreline retreat at P4 is 15 m and maximum shoreline retreat is 30 m.

Discrepancies between video-detected waterlines and field observations were only observed with prominent intertidal bars. Waterlines were not only identified on the seaward slope of intertidal bars, but also in the trough. However, residual water in feeder channels or troughs in the intertidal beach often do not correspond to the mean water level of the adjacent sea. This was not solely caused by the cross-shore gradient in wave set-up, but also by processes like exfiltration of groundwater on the intertidal beach. Overall, the CSIs in this paper provided robust and reliable comparisons with field verification.

A successful CSI is also capable of indicating the evolution of a coastal system with its trends and natural variations. The evolution of video-derived shoreline positions on time scales which embraced storm event were presented for all sites. The morphodynamic impact of storm waves was clearly measurable with all the indicators under investigation. The moment of change in all time series could be resolved to within a day, since the video observations were obtained at high frequency and during extreme conditions. This was certainly not the case in traditionally measured CSIs. Additionally, the video-derived indicators gave much more information about the alongshore variability due to their high spatial resolution.

The evolution of a coastal system as expressed by a CSI over weeks to years was shown in the case of a shoreline on a protected beach (Fig. 6), a spit (Fig. 7) and an unprotected beach (Fig. 8). In all cases, the character of the morphological changes (subtle or abrupt) could be detected with high temporal resolution.

Application of a CSI within a management scheme requires a predefined bench marking procedure. The coastal manager needs to have threshold values for indicators beyond which intervention is required (see Davidson et al., 2007-this edition). The application of video-derived indicators was successful in evaluating the need for, and effectiveness of, human interventions like beach nourishment (Egmond beach) and dredging (El Puntal spit). CSI were successfully developed to monitor the spatial impact and longevity of both nourishment (Fig. 10) and dredging interventions (Fig. 12). These video parameters could also indicate under which conditions the changes occurred, especially if the indicators were evaluated at a daily frequency. The lifetimes of both projects were on the order of half a year and major alongshore variation occurred along both 2 km wide stretches. The temporal resolution of the traditional surveys was insufficient to give a life-time estimate, and the spatial resolution of the traditional surveys was often too low to observe and understand the alongshore variations in the CSIs. These findings indicate that video-derived datasets of CSIs offer significant improvement to current CZM practices.

7. Conclusions

This contribution has assessed the utility of video-derived CSIs for the monitoring and management of coastal stability problems. The principle indicators under investigation were secondary products of shorelines extracted from 10 min time-average images. CSIs included: shoreline contours at a constant pre-defined level, (intertidal) beach volumes, and momentary shoreline positions which reflect the sand volume in a meter wide section of the intertidal coast. In all cases these parameters displayed useful accuracy when compared to traditional monitoring methods. Applications of these CSIs included the study of the natural behaviour of beaches and spits and the impact of storms and seasonal changes, the impact of nourishments and dredging activities on the coastline. In all cases, the indicators used highlighted the trends in coastal evolution and could clearly identify the impact of the natural behaviour and human interventions. Threshold values could be established for each indicator, beyond which intervention could be executed. The Argus video system could estimate the indicators with a much higher resolution in space (sub meter resolution over 1–2 km) and over a broad range of time scales (days, weeks, months, seasons and years) than is practically possible using traditional monitoring techniques. Therefore, it can also: 1) better resolve the time span over which the coastline position changes and couple this to current forcing, 2) indicate the rate of change of coastline behaviour, 3) give an indication of the recovery times of natural systems to impacts by storms or human interventions, and 4) estimate the effectiveness of human interventions.

Acknowledgements

The Argus group is thanked for all the efforts in developing techniques to process video images and to finally derive the CSIs out of the single images. Besides, all technical support of John Stanley (Oregon State University) and Irv Elshoff (WL | Delft Hydraulics) is greatly appreciated. We also want to thank the local acts of assistance rendered by the Ministry of Transport and Public Works (Rijkswaterstaat, directie Noord-Holland) at Egmond beach and by the Santander Port Authority at El Puntal spit. Aart Kroon performed part of his research at Utrecht University, the Netherlands. González wants to express his thanks to the Spanish Ministry of Science and Technology under the Ramón y Cajal Program, and the Spanish Comisión Interministerial de Ciencia y Tecnología (CICYT) under research grant REN2003-9640/MAR. Kathelijne Wijnberg (University of Twente) is thanked for the help with the analysis of the beach nourishment data. Paolo Ciavola (University of Ferrara) is thanked for his efforts in Lido di Dante and Susanne Quartel (Utrecht University) for her efforts in Egmond. Rob Holman would like to thank the Office of Naval Research, Coastal Geosciences program (grant #N00014-02-1-0154) for support of CoastView collaborations. The constructive comments of Philippe Larouddé and Ian Turner on an earlier version of this manuscript were gratefully appreciated.

References

Aagaard, T., Kroon, A., Andersen, S., Møller Sørensen, R., Quartel, S., Vinther, N., 2005. Intertidal beach change during storm conditions, Egmond, The Netherlands. Marine Geology 218 (1–4), 65–80.

Aarninkhof, S.G.J., 2003. Nearshore bathymetry derived from video imagery. PhD-Thesis, Delft University of Technology, Delft, The Netherlands.

Aarninkhof, S.G.J., Caljouw, M., Stive, M.J.F., 2000. Video-based, quantitative assessment of intertidal beach variability. Proc. 27th International Conference of Coastal Engineering 2000. ASCE, pp. 3291–3304.

Aarninkhof, S.G.J., Turner, I.L., Dronkers, T.D.T., Caljouw, M., Nipius, L., 2003. A video-based technique for mapping intertidal beach bathymetry. Coastal Engineering 49 (4), 275–289.

Bender, C.J., 2001. Wave field modifications and shoreline response due to offshore borrow areas. MSc-Thesis, University of Florida, Gainesville, Fla.

Boak, E.H., Turner, I.L., 2005. Shoreline definition and detection: a review. Journal of Coastal Research 21 (4), 688–703.

Ciavola, P., Corbau, C., Cibin, U., Perini, L., 2003. Mapping the coastal zone of the Emilia-Romagna region using geographical information systems. Proceedings of Medcoast Conference, Ravenna, Italy, pp. 2363–2374.

Davidson, M.A., Van Koningsveld, M., De Kruif, A., Rawson, J., Holman, R.A., Lamberti, A., Medina, R., Kroon, A., Aarninkhof, S.G.J., 2007. The CoastView project: developing video-derived coastal state indicators in support of coastal zone management. Coastal Engineering Special Issue of the CoastView project 54, 463–475 (this edition). doi:10.1016/j.coastaleng.2007.01.007.

Demir, H., Otay, E.N., Work, P., Borëkçi, 2004. Impacts of dredging on shoreline change. Journal of Waterway, Port, Coastal and Ocean Engineering 130 (4), 170–178.

Hamm, L., Capobianco, M., Dette, H.H., Lechuga, A., Spanhoff, R., Stive, M.J.F., 2002. A summary of European experience with shore nourishment. Coastal Engineering 47 (2), 237–263.

Hanson, H., Brampton, A., Capobianco, M., Dette, H.H., Hamm, L., Laustrup, C., Lechuga, A., Spanhoff, R., 2002. Beach nourishment projects, practices, and objectives-a European overview. Coastal Engineering 47 (2), 81–111.

Holland, K.T., Holman, R.A., Lippmann, T.C., 1997. Practical use of video imagery in nearshore oceanographic field studies. IEEE Journal of Oceanic Engineering 22 (1), 81–92.

Holman, R.A., Stanley, J., 2007. The history, capabilities and future of Argus. Coastal Engineering Special Issue of the CoastView project 54, 477–491 (this edition). doi:10.1016/j.coastaleng.2007.01.003.

Holman, R.A., Sallenger Jr, A.H., Lippmann, T.C., Haines, J.W., 1993. The application of video image processing to the study of nearshore processes. Oceanography 6 (3), 78–85.

Horikawa, K., Sasaki, T., Sakuramoto, H., 1977. Mathematical and laboratory models of shoreline changes due to dredged holes. Journal of the Faculty of Engineering University, Tokyo 34 (B), 49–57.

Kroon, A., De Boer, A.G., Degruyse, C., Levoy, F., Meesen, B.M., Ruessink, B.G., 2002. Beach morphodynamics. In: Van Rijn, L.C., Ruessink, B.G., Mulder, J.P.M. (Eds.), COAST3D-Egmond, The Behaviour of a Straight Sandy Coast on the Time Scale of Storms and Seasons. Aqua Publications, pp. M1–M16.

Lippmann, T.C., Holman, R.A., 1989. Quantification of sand bar morphology: a video technique based on wave dissipation. Journal of Geophysical Research 94 (C1), 995–1011.

Losada, M.A., Medina, R., Vidal, C., Roldan, A., 1991. Historical evolution and morphological Analysis of "El Puntal" Spit, Santander (Spain). Journal of Coastal Research 7 (3), 711–722.

Medina, R., Marino-Tapia, I., Osorio, A., Davidson, M., Martin, F.L., 2007. Management of dynamic navigational channels using video techniques. Coastal Engineering Special Issue of the CoastView project 54, 523–537 (this edition). doi:10.1016/j.coastaleng.2007.01.008.

Plant, N.G., Holman, R.A., 1997. Intertidal beach profile estimation using video images. Marine Geology 140 (1–2), 1–24.

Plant, N.G., Holland, K.T., Puelo, J.A., 2002. Analysis of the scale errors in nearshore bathymetric data. Marine Geology 191 (1–2), 71–86.

Ruessink, B.G., Kroon, A., 1994. The behaviour of a multiple bar system in the nearshore zone of Terschelling, The Netherlands. Marine Geology 121 (3–4), 187–197.

Sallenger, A.H., Krabill, W., Swift, R., Brock, J., List, J., Hansen, M., Holman, R.A., Manizade, S., Sontag, J., Meredith, A., Morgan, K., Yunkel, J.K., Frederick, E., Stockdon, H., 2003. Evaluation of airborne scanning lidar for coastal change applications. Journal of Coastal Research 19 (1), 125–133.

Smit, M.W.J., Aarninkhof, S.G.J., Wijnberg, K.M., Gonzalez, M., Kingston, K.S., Southgate, H.N., Ruessink, B.G., Holman, R.A., Siegle, E., Davidson, M., Medina, R., 2007. The role of video imagery in predicting daily to monthly coastal evolution. Coastal Engineering Special Issue of the CoastView project 54, 539–553 (this edition). doi:10.1016/j.coastaleng.2007.01.009.

Spanhoff, R., Biegel, E.J., Van der Graaff, J., Hoekstra, P., 1997. Shoreface nourishment at Terschelling, The Netherlands: feeder berm or breaker berm? Proceedings of the Coastal Dynamics '97, Plymouth, UK, pp. 863–872.

Stockdon, H., Sallenger, A.H., Holman, R.A., List, J., 2002. Estimation of shoreline position and change from airborne scanning lidar data. Journal of Coastal Research 18 (3), 502–513.

Siegle, E., Huntley, D.A., Davidson, M.A., 2002. Modelling water surface topography at a complex inlet system Teignmouth, UK. Journal of Coastal Research SI 36, 676–685.

Simons, R., Hollingham, S., 2001. Marine aggregate dredging: a review of current procedures for assessing coastal processes and impact at the coastline. Technical Rep. HYD10401, Civil and Environmental Engineering Department. Univ. College of London, London, UK.

Turner, I.L., Anderson, D.J., 2007. Web-based and 'real-time' beach management system. Coastal Engineering Special Issue of the CoastView project 54, 555–565 (this edition). doi:10.1016/j.coastaleng.2007.01.002.

Turner, I.L., Aarninkhof, S.G.J., Dronkers, T.D.T., McGrath, J., 2004. CZM applications of Argus coastal imaging at the Gold Coast, Australia. Journal of Coastal Research 20 (3), 739–752.

Van Duin, M.J.P., Wiersma, N.R., Walstra, D.J.R., Van Rijn, L.C., Stive, M.J.F., 2004. Nourishing the shoreface: observations and hindcasting of the Egmond case, The Netherlands. Coastal Engineering 51 (8–9), 813–837.

Van Enckevort, I.M.J., Ruessink, B.G., 2003. Video observations of nearshore bar behaviour. Part 2: Alongshore non-uniform variability. Continental Shelf Research 23 (5), 513–532.

Van Koningsveld, M., 2003. Matching specialist knowledge with end user needs. PhD-Thesis, University of Twente, Enschede, The Netherlands.

Van Koningsveld, M., Mulder, J.P.M., 2004. Sustainable coastal policy developments in The Netherlands. A systematic approach revealed. Journal of Coastal Research 20 (2), 375–385.

Wijnberg, K.M., Terwindt, J.H.J., 1995. Quantification of decadal morphological behaviour of the central Dutch coast. Marine Geology 126 (1–4), 301–330.

Wijnberg, K.M., Kroon, A., 2002. Barred beaches. Geomorphology 48 (1–3), 103–120.

Wijnberg, K.M., Aarninkhof, S.G.J., Van Koningsveld, M., Ruessink, B.G., Stive, M.J.F., 2004. Video monitoring in support of coastal management. Proc. 29th International Conference on Coastal Engineering 2004. ASCE. 13 pp.

Work, P.A., Fehrenbacher, F., Voulgaris, G., 2004. Nearshore impacts of dredging for beach nourishment. Journal of Waterway, Port, Coastal and Ocean Engineering 130 (6), 303–311.